SAGE CRISP PUBLICATIONS DIRECTORY

Authors:-

Al-Tabbaa, A. and Muir Wood, D.

HORIZONTAL DRAINAGE DURING CONSOLIDATION: INSIGHTS GAINED FROM ANALYSIS OF A SIMPLE PROBLEM

Publication:-

GEOTECHNIQUE VOLUME 41, NO 4, pp 571-585

Year of Publication:-

1991

Al-Tabbaa, A. & Muir Wood, D. (1991). *Géotechnique* 41, No. 4, 571–585

Horizontal drainage during consolidation: insights gained from analyses of a simple problem

A. AL-TABBAA* and D. MUIR WOOD†

This paper analyses consolidation with radial drainage to concentric inner and outer fixed drainage boundaries. An analysis in which coupling between flow of pore water and effective stress change is ignored gives results that are not physically reasonable. An exact closed form solution can be developed to the equation of radial pore water diffusion in an elastic material and the results of this analysis are compared with a third, finite element analysis, using an elastic–plastic description of the soil. Elastic and elastic–plastic analyses are compared in terms of isochrones of pore pressure, radial displacement and stress change within the sample, and in terms of the strain and stress paths followed by different soil elements in the consolidating clay. Non-uniformities of effective stress state, and hence of soil stiffness, can develop during consolidation; the pattern of deformations that develops is completely dominated by the occurrence of plastic strains. The oedometer should not be regarded as a single element test. The results of the analyses are in principle specific to the boundary conditions assumed, but some general aspects of soil behaviour are identified and observations are made on the implications of the results for geotechnical design.

KEYWORDS: consolidation; numerical modelling and analysis; clays; elasticity; plasticity; permeability.

L'article présente une analyse de la consolidation avec drainage radial jusqu'à des limites de drainage intérieure et extérieure fixes. Une analyse qui ignore le couplage entre l'écoulement de l'eau interstitielle et des changements dans la contrainte effective donnent des résultats qui ne sont pas physiquement raisonnable. L'équation de la diffusion radiale de l'eau interstitielle dans une matière élastique peut être résolue dans une forme fermée précise. Les résultats de cette analyse sont comparés avec une analyse à éléments finis employant une description élastico–plastique pour l'argile. Les analyses élastique et élastico-plastique sont comparées en ce qui concerne les isochrones de la pression de l'eau interstitielle, le déplacement radial, le changement des contraintes dans l'échantillon et aussi les chemins de contrainte et de déformation suivis par de différents éléments dans l'argile pendant la consolidation. Un état de contrainte effective et par conséquent de rigidité de sol qui est non-uniforme peut se développer au cours de la consolidation. Le système de déformations qui se développe est régi par la présence de contraintes plastiques. Il ne faut pas considérer l'oedomètre comme un essai à élément simple. En principe les résultats de l'analyse sont spécifiques pour les conditions limites, mais des aspects généraux du comportement des sols sont identifiés et des observations faites concernant les implications des résultats pour la construction géotechnique.

INTRODUCTION

Horizontal drainage is important in many geotechnical situations involving consolidation. As horizontal permeabilities are typically larger than vertical permeabilities, horizontal drainage often predominates. Despite its importance, the problem of consolidation with horizontal drainage is not well understood. For example, the time-dependent non-uniform vertical strains which result from horizontal drainage under a flexible structure, and the residual non-uniformity in stresses and strains at the end of consolidation under a rigid structure which results from plastic deformation of the soil, may produce stresses in structures founded on consolidating ground that were not envisaged by the designer. This paper does not provide detailed guidance, but translates the findings of a detailed study of a simple problem, in the broadest terms, into general statements that may assist the designer. As the modes of behaviour observed will depend to a large extent on the soil description used, some sets of analyses are performed and compared, so that the influence of the soil model may be ascertained.

The problem chosen for detailed study is the consolidation of a block of soil with radial drainage to concentric inner and outer fixed drainage

Discussion on this Paper closes 1 April 1992; for further details see p. ii.

* University of Birmingham.
† University of Glasgow.

boundaries. The block of soil is confined between rigid horizontal platens, so that vertical deformation following the application of a vertical load is uniform at all radii.

In a conventional oedometer, samples of clay are compressed vertically between rigid platens, flow of water occurs vertically upwards or downwards towards drainage surfaces in these platens, and experimental observations are interpreted to give a one-dimensional coefficient of vertical consolidation and a permeability for vertical flow of water through the clay soil. Rates of settlement of geotechnical structures are frequently controlled by the rate at which excess pressures can dissipate to the sides of those structures; this rate is governed by the horizontal permeability of the soil, which may typically be several times larger than the vertical permeability.

To allow estimation of the horizontal permeability of clays such as speswhite kaolin, which are used in many laboratory and centrifuge model tests, a modification to a conventional oedometer was devised by Al-Tabbaa & Wood (1987) in which, though the clay sample is again compressed vertically between rigid platens, flow of water occurs radially to concentric internal and external drainage boundaries (Fig. 1). With this apparatus, values of horizontal permeability can be estimated both from falling head tests conducted with a head difference between the two drainage boundaries, and, in principle, from analysis of the time-dependent deformations occurring during any increment of load.

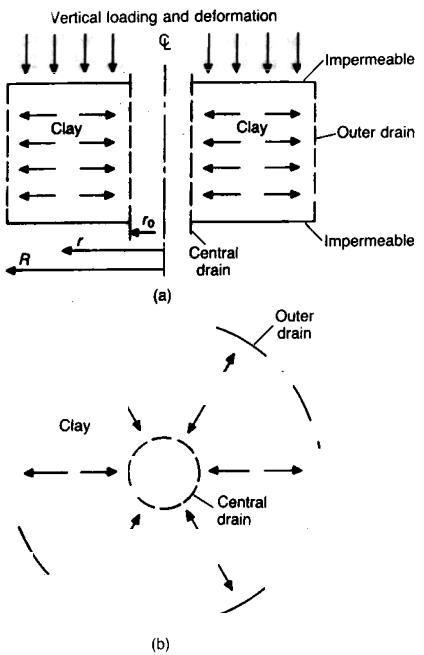

Fig. 1. Oedometer with radial drainage: (a) section; (b) plan

Analysis of the time-dependent deformations requires solution of the equation of pore water diffusion for the case of radial flow to inner and outer boundaries. Carslaw & Jaeger (1959) state the solution for the essentially similar problem of flow of heat through a conducting medium, but do not present any numerical results. For the geotechnical application of pore water diffusion, Barron (1948) studies the problem of radial flow inwards to a sand drainage column, while McKinlay (1961) develops the solution for consolidation of a solid cylindrical sample with flow of water to an outer drainage boundary only. Randolph & Wroth (1979) and Randolph & Carter (1979) have produced results for the consolidation that occurs around an impermeable or permeable driven pile as a result of the dissipation of excess pore pressures set up during the driving of the pile. The Authors are not aware of a previous presentation of numerical results for the situaton of radial flow between two concentric boundaries, for which McKinlay's solution and the solution for conventional one-dimensional (vertical) consolidation provide limiting cases corresponding to ratios of radii equal to 0 and 1 respectively.

The results of two analyses are contrasted below. In both, the flow of pore water and deformation of the soil are fully coupled. The soil is described in one as an isotropic elastic material, and in the other using the modified Cam clay elastic–plastic constitutive model. Although the impetus to undertake this study came from an associated series of experiments, this Paper is concerned only with the findings of the analyses. The phenomena that the analytical studies have revealed could, in principle, be tested by instrumentation of laboratory oedometers, and in particular by measurement of internal pore pressures, but this was not possible in the small (88 mm dia.) oedometer used by Al-Tabbaa & Wood (1987) for their permeability measurements.

ANALYSIS

Because the deformation of the soil in this problem is so kinematically constrained by rigid fixed and moving boundaries, it is tempting to perform an uncoupled analysis in which all the soil, at all radii in the oedometer, deforms uniformly and one-dimensionally, vertically, matching the imposed boundary deformation. The radial distribution of pore pressure which is

required to drive the radial flow associated with the changes in volume of the one-dimensionally compressing soil can be calculated analytically. However, as shown in Appendix 1, this analysis leads to a physically unrealistic requirement for a finite, non-zero, strain rate at zero time.

If the condition of one-dimensional internal deformation is relaxed and soil elements within the oedometer are allowed to move radially as well as vertically, then a fully coupled Biot solution can be obtained in which the deformation of the soil elements is linked with the changing three-dimensional effective stress state in the soil, changes in effective stress are linked with changes in pore pressure, and changes in pore pressure are linked through Darcy's law with the volume changes resulting from the deformation of the soil. The following assumptions are common to all the analyses.

(*a*) The soil is homogeneous and fully saturated.
(*b*) The pore water and soil particles are incompressible.
(*c*) The flow of water down a radial gradient of excess pore pressure is governed by Darcy's law, with a constant horizontal permeability k_h during a given stage of consolidation.

The analyses are also governed by the following boundary conditions.

(*a*) The soil is laterally confined so that no radial movement can occur at either the inner or outer boundary.
(*b*) Drainage occurs at the inner and outer boundaries so that the excess pore water pressure at these radii is always zero.
(*c*) The soil is contained vertically between rigid platens so that the vertical strain is a function only of time and not of radius. The vertical strain ε_z is zero at $t = 0$ and tends towards its final value ε_∞ as time increases towards infinity.
(*d*) For all radii, the radial movement, excess pore pressure and vertical strain are initially zero.
(*e*) The consolidation of the sample is driven by an increment of total vertical load ΔP which remains constant with time and whose non-uniform distribution with radius is such that the condition of uniform vertical strain is maintained across the sample.

A closed-form analytical solution to this fully coupled problem can be obtained provided that the soil is described as incrementally elastic. Details of the analysis for an isotropic elastic soil are given in Appendix 1. The elastic analysis is performed using the volumetric strain V, which is a function only of radius r, as the independent variable. Once the radial distribution of V has been obtained, expressions can be deduced for the pore pressure u and the radial movement ξ, and hence for the radial and circumferential strains, as functions of radius.

Stresses can be calculated using Hooke's law with the previously calculated strains, but it is more convenient to obtain the stresses from numerical analysis using a finite element program. Both of the numerical analyses described below were performed using the CRISP finite element program (Britto & Gunn, 1987). In these analyses the loading and drainage conditions have been chosen to correspond to those of a particular real situation studied experimentally in a modified oedometer (Al-Tabbaa & Wood, 1987). The loading is chosen to increase the total vertical load by 10% of its initial value; this is the average vertical stress increment ratio used in the experiments summarized by Al-Tabbaa and Wood. The layout of the finite element mesh used for both analyses is shown in Fig. 2. The displacements and strains computed for the first (elastic) analysis have been compared with the theoretical closed-form elastic solution in order to validate the finite element approximation. Details of this validation are given by Al-Tabbaa (1987).

Normally-compressed clay can be better described as elastic–plastic than as incrementally isotropic elastic. Consolidation of elastic–plastic soil is readily studied by numerical analysis. In the second analysis, the modified Cam clay model (Roscoe & Burland, 1968) is used to describe the behaviour of the soil. Appropriate soil parameters for the speswhite kaolin clay used in the associated experimental programme of triaxial stress path tests (Al-Tabbaa, 1987) are used: these are summarized in Appendix 2. It is assumed that, at the start of the load increment under study, the soil is uniformly stressed at all radii, with the same initial size of yield locus.

It is convenient to present some of the results of the analyses in terms of non-dimensional

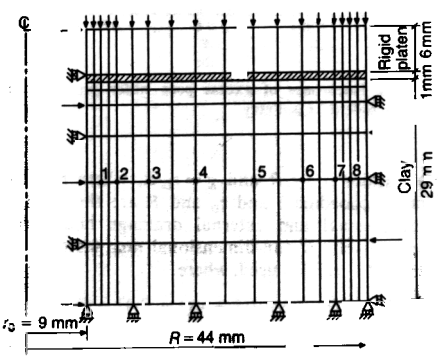

Fig. 2. Finite element mesh

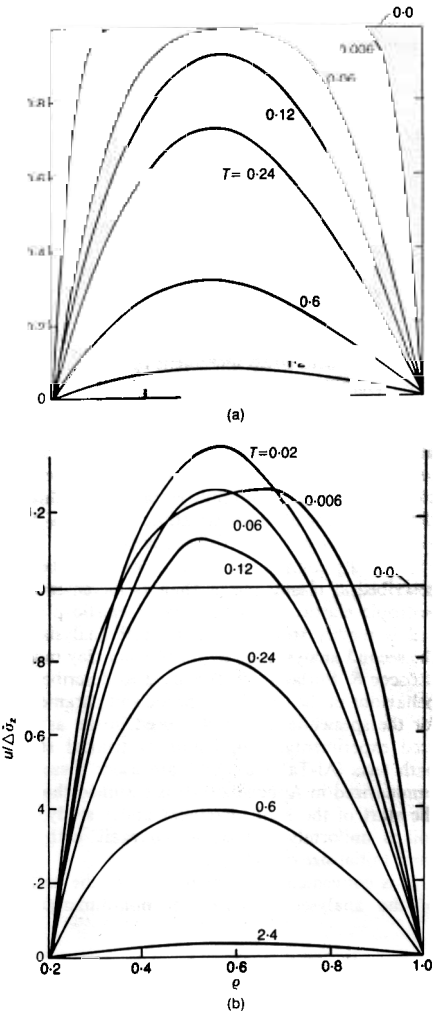

Fig. 3. Isochrones of excess pore water pressure: (a) elastic soil; (b) Cam clay

quantities $\rho = r/R$ and $\chi = r_0/R$, where r is the radial coordinate and r_0 and R are the radii of the internal and external drainage boundaries respectively. A non-dimensional time factor $T = 4ct/[(R - r_0)^2]$ is used, where

$$c = k_h E(1 - \nu)/\gamma_w[(1 + \nu)(1 - 2\nu)] = k_h m_v/\gamma_w$$

is introduced as an appropriate coefficient of consolidation (see Appendix 1). For the elastic–plastic Cam clay analysis the value of c is chosen to give an approximate equivalence of volumetric stiffnesses. For both the elastic and the Cam clay analyses a value of $T = 1$ implies a time since the start of consolidation of 500 s. Most results are shown for the specific case $\chi = 0{\cdot}205$, which corresponds with the experimental situation.

Isochrones of excess pore pressure (Fig. 3)

The pore pressures are normalized by dividing by the applied increment of average total vertical stress $\Delta\bar{\sigma}_z$. The uncoupled Terzaghi analysis gives unreasonable results when the soil is assumed to be subjected to uniform vertical *strain* at all radii. An uncoupled analysis can also be performed for the different situation of a soil sample subjected to a uniform vertical total *stress* at all radii. In the latter case, the differential equation governing the variation of either volumetric strain or pore pressure with radius and time is identical in form to equation (26), which governs the variation of volumetric strain V with radius and time for the fully coupled analysis. The isochrones of excess pore pressure for the coupled elastic analysis (Fig. 3(a)) are therefore identical to those that would be deduced for this alternative uncoupled analysis. The pore pressure decays steadily from the initial uniform distribution, with the first harmonic of the radial distribution rapidly becoming dominant.

In contrast, the Cam clay analysis shows an initial rise in pore pressure away from the drainage boundaries, to a value $\sim 30\%$ higher than the initial uniform value (Fig. 3(b)). Although the 'first harmonic' again rapidly becomes dominant, the eventual decay back to zero is slower than for the elastic soil.

Isochrones of volumetric strain (Fig. 4)

The volumetric strains are normalized by dividing by the final volumetric strain V_∞ which, for the Cam clay analysis, is the average volumetric (and vertical) strain at the end of consolidation. The isochrones of volumetric strain for the elastic analysis (Fig. 4(a)) are identical to the isochrones of excess pore pressure (Fig. 3(a)). For Cam clay (Fig. 4(b)) the soil near the drainage boundaries compresses rapidly to begin with, but the subsequent volumetric strain is rather uniform at all radii. When the pore pressure has been completely dissipated, the overall effect is to leave the soil with a small radial variation of specific volume.

Isochrones of vertical stress (Fig. 5)

The analyses are performed with a constant total load applied to the rigid top platen.

However, the deformation of the soil and the resulting pore pressure changes lead to variations with radius of total vertical stress. These variations are shown in Fig. 5(a and c) for the elastic and Cam clay analyses respectively. For the elastic soil (Fig. 5(a)) the variation in total stress away from the drainage boundaries is not great, and the variation in vertical effective stress (Fig. 5(b)) is consequently rather similar to the variation of pore pressure. At large values of time, the total and effective vertical stresses are once again uniform.

The variations in total stress are much greater for Cam clay (Fig. 5(c)), and the isochrones of vertical effective stress (Fig. 5(d)) are rather similar to those of volumetric strain (Fig. 4(b)). In the Cam clay analysis, both the total and the effective vertical stresses ultimately vary non-uniformly with radius.

Isochrones of radial displacement (Fig. 6)

The radial displacements are plotted non-dimensionally in terms of $\xi/V_\infty r_0$ in Fig. 6, where, for the Cam clay analysis, the final volumetric strain V_∞ is the average volumetric (and vertical) strain at the end of consolidation. It should be noted that the scales chosen are different for the elastic soil (Fig. 6(a)) and the Cam clay (Fig. 6(b)). For both soils movements occur towards each drainage boundary, but whereas the elastic soil moves back to its original position, leaving no net radial displacement, the radial movement that occurs initially is locked into the Cam clay and is not recovered. The amounts of non-dimensional radial movement are much smaller for Cam clay than for the elastic soil.

Stress and strain paths (Figs 7 and 8)

The isochrones showing radial distributions of several variables in Figs 3–6 provide a natural way of comparing the results of the two analyses. However, the differences between the two analyses can be explained more easily by studying the patterns of stress and strain paths followed at various radii. Although plots of stress and strain paths may be unfamiliar, they illustrate the fundamental differences in the nature of the stress–strain response of elastic and elastic–plastic soils.

The symmetries of the problem are such that the vertical, radial, and circumferential stresses will be principal stresses at all times, but in general no two of the three stresses will be equal, so that stress variables used to display stress changes that may be applied in the conventional triaxial apparatus are not directly useful. In the conventional triaxial apparatus it is usually assumed that radial and circumferential stresses

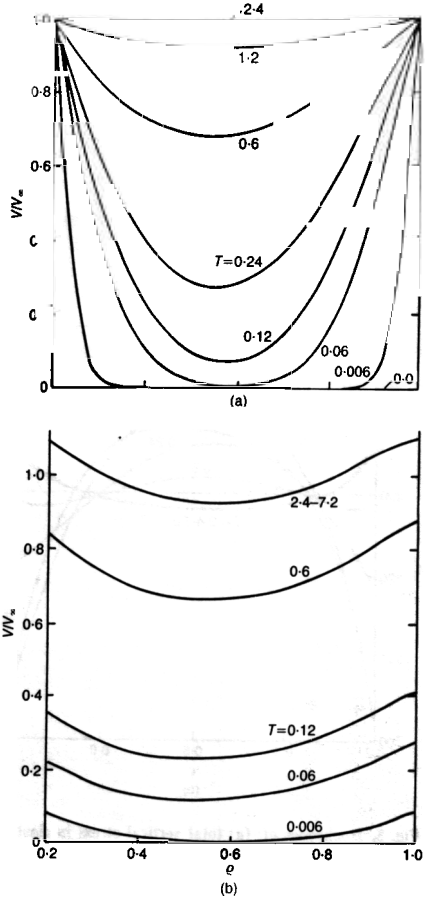

Fig. 4. Isochrones of volumetric compressive strain: (a) elastic soil; (b) Cam clay

are equal ($\sigma_\theta' = \sigma_r'$), and triaxial stress paths are presented in terms of deviator stress $q = \sigma_z' - \sigma_r'$ and mean effective stress $p' = (\sigma_z' + 2\sigma_r')/3$ (Wood, 1984). In the present radial consolidation problem the initial stress state has equal radial and circumferential stresses, and the vertical stress remains the major principal stress at all times. The stress changes accompanying the consolidation process can be regarded as a perturbation from this initially axisymmetric stress state. It is natural, therefore, to present part of the stress path information in a plot of $q = (2\sigma_z' - \sigma_\theta' - \sigma_r')/2$ and $p' = (\sigma_z' + \sigma_\theta' + \sigma_r')/3$. The variable $q = (2\sigma_z' - \sigma_\theta' - \sigma_r')/2$ is closely similar to the deviator stress (and is identical to it for $\sigma_\theta' = \sigma_r'$),

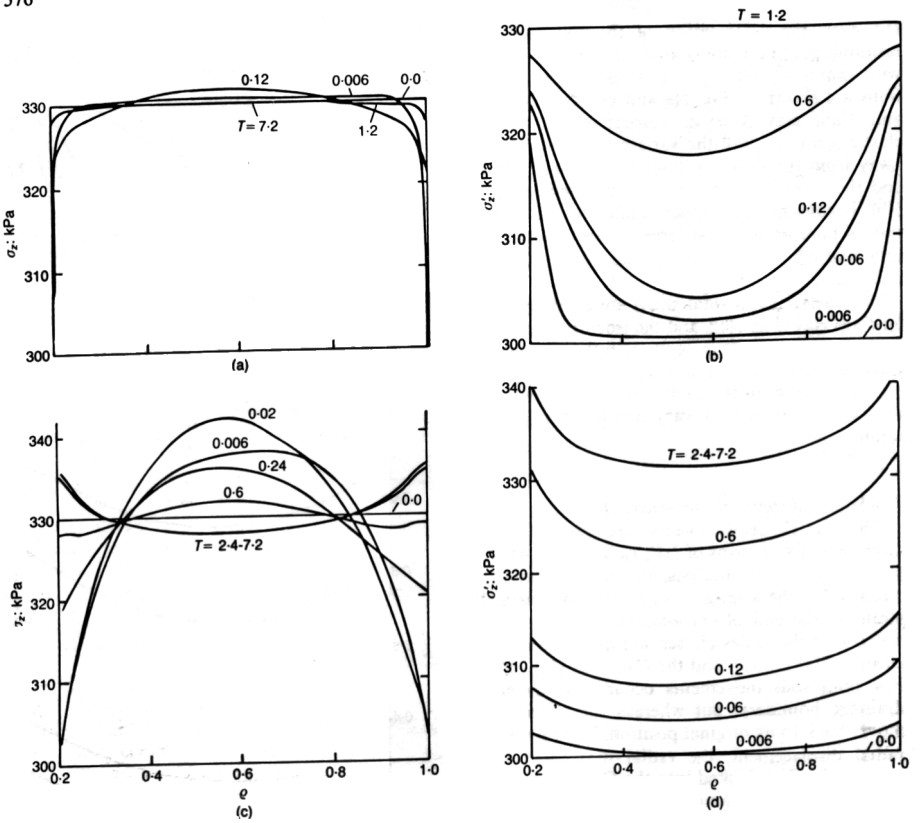

Fig. 5. Isochrones of: (a) total vertical stress in elastic soil; (b) effective vertical stress for (a) in elastic soil; (c) total vertical stress in Cam clay; (d) effective vertical stress in Cam clay

and the variable $p' = (\sigma_z' + \sigma_\theta' + \sigma_r')/3$ is the mean effective stress defined for the more general stress state that is appropriate here (and is again identical for $\sigma_\theta' = \sigma_r'$). A mean total stress $p = (\sigma_z + \sigma_\theta + \sigma_r)/3$ can be defined in terms of the total stresses; clearly it makes no different whether q is defined in terms of total or effective stresses. Total and effective stress paths are plotted for the elastic soil and for Cam clay in terms of q and p and p' in Fig. 7(a) and (c) respectively. Paths are plotted for eight points across the sample; the locations of these points are shown in Fig. 2. Note that, in order to show the stress changes more clearly, the scales used for the general deviator stress q in Fig. 7(a) and (c) differ by a factor of 2.

The $q : p'$ plot contains only two of the three dimensions needed to present the complete stress information. The definition of q absorbs differences between radial and circumferential stresses; thus a natural second plot to use is of q and $x = (\sigma_r' - \sigma_\theta')$. As both variables now involve differences of principal stresses only, it does not matter whether they are calculated in terms of total or effective stresses, and the total and effective stress paths in this plot are identical. Plots of the $q : x$ stress paths for the elastic soil and for Cam clay are shown in Fig. 7(b) and (d) respectively. (The scales have been chosen in Fig. 7(b) and (d) so that these plots represent the deviatoric or π-plane view of principal stress space.)

The strain paths can be displayed in terms of equivalent variables: volumetric strain $(\varepsilon_z + \varepsilon_r + \varepsilon_\theta)/V_\infty$, a deviator strain $(2\varepsilon_z - \varepsilon_r - \varepsilon_\theta)/V_\infty$, and a strain difference $(\varepsilon_r - \varepsilon_\theta)/V_\infty$. Strain paths for the elastic soil and for Cam clay are shown in terms of these variables in Fig. 8(a) and (b) and Fig. 8(c) and (d) respectively. Again, for the Cam

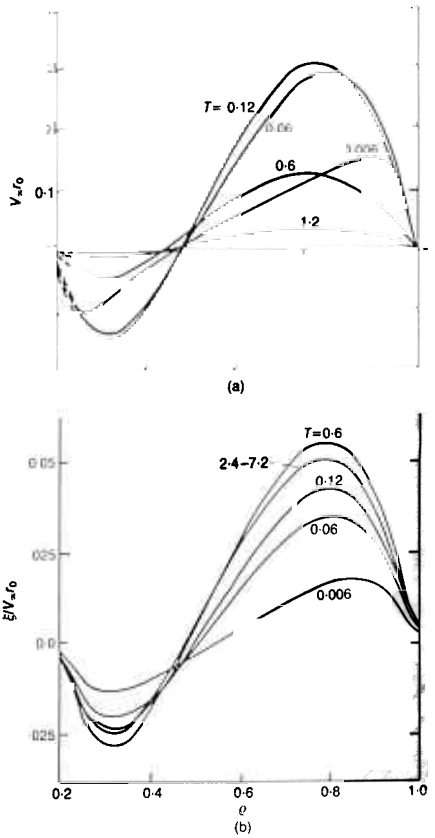

Fig. 6. Isochrones of radial movement: (a) elastic soil; (b) Cam clay

clay analysis, the final volumetric strain V_∞ is the average volumetric (and vertical) strain at the end of consolidation.

DISCUSSION

Stress and strain paths

For the elastic soil the stress state of all elements starts at the same point and ends at the same point. There is a spread of routes by which the starting and ending points are linked, but these two points lie on the one-dimensional elastic compression path for the soil. The same end point would be attained if the elastic soil were loaded in a conventional oedometer with purely vertical drainage and flow. The total stress paths shown at the right-hand side of Fig. 7(a) also show a spread of routes between the starting and finishing points, with the total mean stress falling slightly in the process: the total vertical stress has the same value at all radii at the start and the same value at all radii at the end of the consolidation (Fig. 5(a)).

The elastic response shown in Figs 7(a) and 8(a) can be summarized as follows. Near the drainage boundaries (points 1 and 8), rapid early dissipation of excess pore pressure is associated with volumetric compression and increase in mean effective stress p'. Away from these boundaries the soil initially remains essentially undrained, and the volumetric compression near the boundaries implies a fall of radial effective stress and an increase in shear stress q and associated shear strain.

For an elastic material, the stress increments and strain increments are directly related for all possible changes in effective stress, and the effective stress paths and strain paths are broadly similar in shape. (compare Fig. 7(a) and (b) with Fig. 8(a) and (b)). For Cam clay they are quite different. Cam clay describes the soil as an elastic–plastic material. Elastic strains will accompany all changes of effective stress, and the rules governing these are the same as for the purely elastic soil. However, if the effective stress change is such that yielding of the soil occurs, plastic strains will result. The rules governing these plastic strains are totally different from those governing the elastic strains. The *magnitude* of the plastic strain increment is controlled by the magnitude of the effective stress increment, but the *relative proportions* of the various components of plastic strain (radial, circumferential, vertical) are controlled by the effective stress state at which yielding occurs. The relative proportions of plastic strain components can be called the mechanism of plastic deformation, and according to the Cam clay model this mechanism is entirely dependent on the stress ratio ($\sim q/p'$) at which yielding is occurring. (A detailed discussion of the way in which strains are generated according to the Cam clay model is provided by Muir Wood (1991).)

At the start of the consolidation process the clay is all in a normally compressed state with the initial effective stresses sitting on the initial yield surface. A section through this initial yield surface is shown in Fig. 7(c). The changes of stress and strain in the elastic–plastic soil are being driven by the same external constraints as for the elastic soil. It may therefore be supposed that the soil would 'like', if it could, to undergo the same sorts of strains, with volumetric compression dominating near the drainage boundaries and distortion more significant in the centre of the soil mass. However, none of the elastic strain paths shown in Fig. 8(a) and (b) is compatible with effective stress changes moving elastically towards the

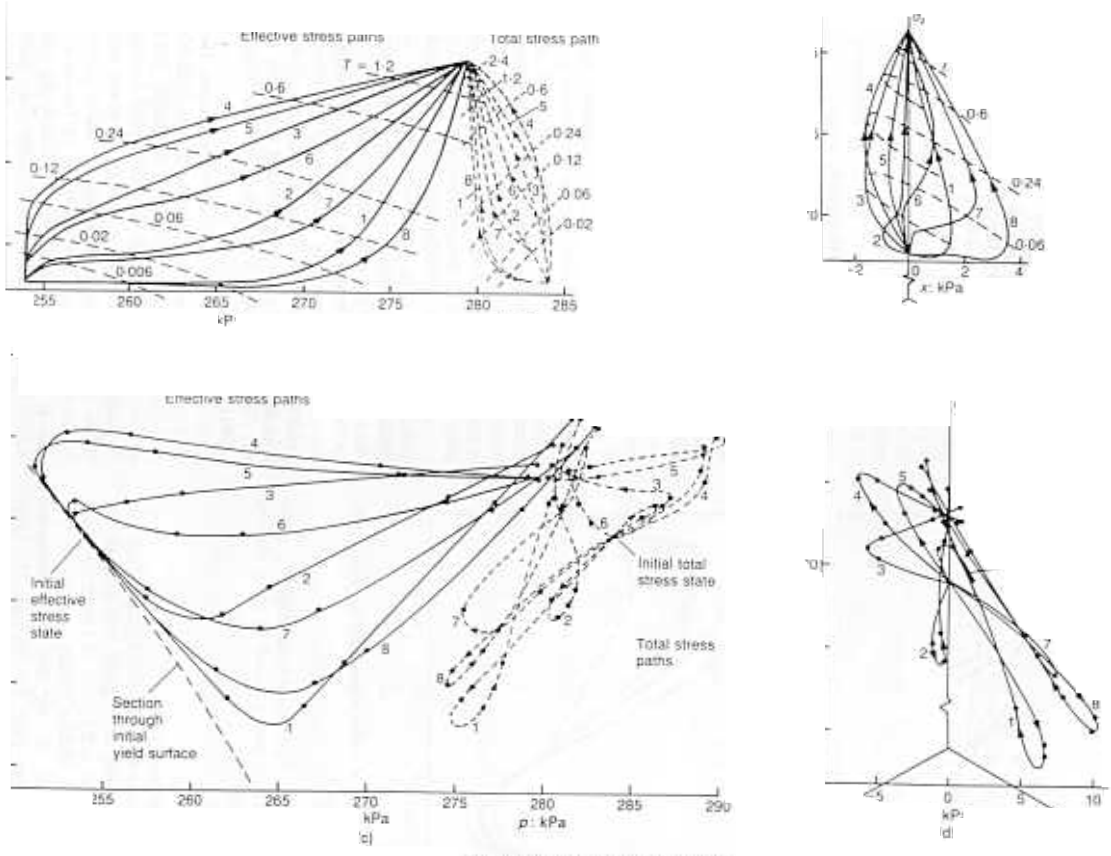

Fig. 7. Total and effective stress paths for soil elements at various radii (see Fig. 2) shown in terms of mean stress $p' = (\sigma_z' + \sigma_\theta' + \sigma_r')/3$ and $p = (\sigma_z + \sigma_\theta + \sigma_r)/3$ and deviator stress $q = (2\sigma_z' - \sigma_\theta' - \sigma_r')/2$ for elastic soil; (b) two deviator stresses q and $x = (\sigma_z' - \sigma_\theta')$ (π plane) for elastic soil; (c) mean stress $p' = (\sigma_z' + \sigma_\theta' + \sigma_r')/3$ and $p = (\sigma_z + \sigma_\theta + \sigma_r)/3$ and deviator stress $q = (2\sigma_z' - \sigma_\theta' - \sigma_r')/2$ for Cam clay; (d) deviator stresses q and $x = (\sigma_z' - \sigma_\theta')$ (π plane) for Cam clay. For Cam clay analysis • indicates times $T = 0{\cdot}006, 0{\cdot}06, 0{\cdot}12, 0{\cdot}6, 2{\cdot}4$

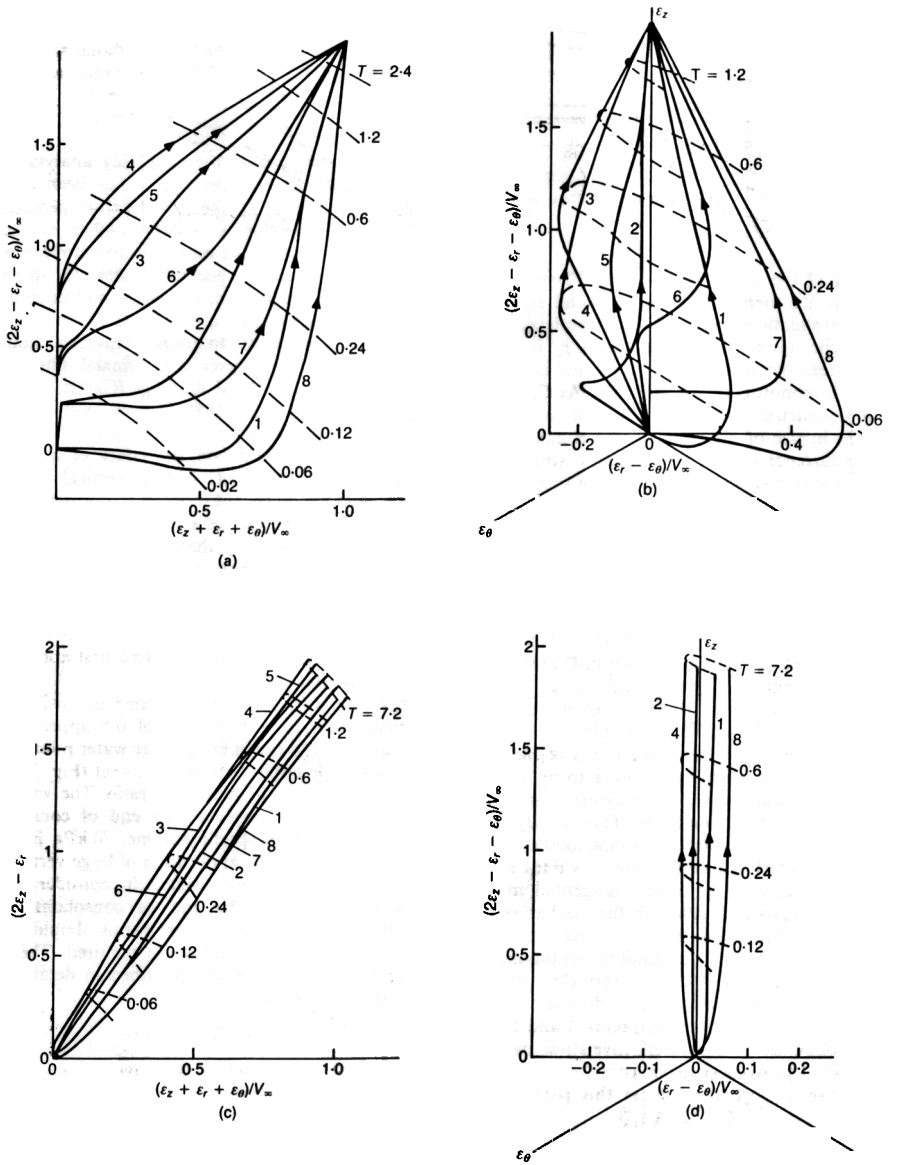

Fig. 8. Strain paths for soil elements at various radii (see Fig. 2) shown in terms of: (a) volumetric strain $(\varepsilon_z + \varepsilon_\theta + \varepsilon_r)/V_\infty$ and deviator strain $(2\varepsilon_z - \varepsilon_\theta - \varepsilon_r)/V_\infty$ for elastic soil; (b) two deviator strains $(2\varepsilon_z - \varepsilon_\theta - \varepsilon_r)/V_\infty$ and $(\varepsilon_r - \varepsilon_\theta)/V_\infty$ (π plane) for elastic soil; (c) volumetric strain $(\varepsilon_z + \varepsilon_\theta + \varepsilon_r)/V_\infty$ and deviator strain $(2\varepsilon_z - \varepsilon_\theta - \varepsilon_r)/V_\infty$ for Cam clay; (d) two deviator strains $(2\varepsilon_z - \varepsilon_\theta - \varepsilon_r)/V_\infty$ and $(\varepsilon_r - \varepsilon_\theta)/V_\infty$ (π plane) for Cam clay

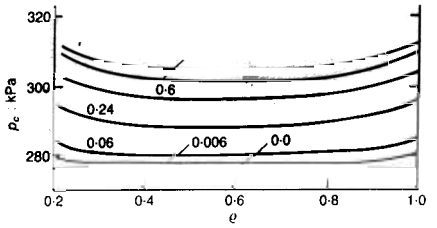

Fig. 9. Isochrones of current size p_c' of Cam clay yield surface

interior of the initial yield surface. Plastic deformations are therefore important at all stages of the consolidation process. This is emphasized by the isochrones of p_c' shown in Fig. 9: p_c' indicates the current size of the yield surface and is seen to increase monotonically at all radii. As Cam clay is a volumetric hardening model, in which the change in size of the yield surface is linked with the occurrence of plastic volumetric strain, it is not surprising that the isochrones of size of yield surface p_c' (Fig. 9) are very similar to the isochrones of volumetric strain (Fig. 4(b)).

Initially the effective stress state is the same at all radii, therefore the mechanism of plastic deformation must be the same at all radii. Even during the consolidation process the stress ratio does not vary greatly through the sample (Fig. 7(c)). Consequently, the strain paths shown in Fig. 8(c) and (d) show very little spread, and are all almost parallel, except at the very start of the consolidation process. It is at this stage that the soil has to escape from the severe limitations of the prescribed plastic mechanism in order to be able to survive the changes in pore pressure that occur near the drainage boundaries. This is only possible if the elastic contributon to the total strain is significant, which will be the case only if the effective stress changes are almost tangential to the yield surface, so that although the mechanism of plastic deformation is fixed, the magnitude of plastic strains is low. This initial tangential movement of the effective stresses is very clear in Fig. 7(c). The associated fall in mean effective stress p' in the middle of the sample (points 4 and 5 virtually follow an undrained effective stress path to begin with) provides a major contribution to the initial rise in pore pressure in this part of the sample.

The total stress paths (right-hand side of Fig. 7(c)) and the deviatoric paths (Fig. 7(d)) are much more tortuous for Cam clay than they were for the elastic soil. This is largely the result of the initial drop in deviator stress q that occurs near the drainage boundaries at the start of the consolidation. It has already been seen that the vertical stress, volumetric strain, and radial displacement are not uniform with radius at the end of consolidation; the stress paths end up at a spread of effective stress states, and the deviatoric plot $q : x$ (Fig. 7(d)) shows that the radial and circumferential stresses are not equal in the end.

Further analyses

The net result from the Cam clay analysis is that the initially uniform sample has been rendered non-uniform by the consolidation process. The specific volume is ~0·004 higher in the centre of the sample, the mean effective stress p' is ~4 kPa lower, and the generalized deviator stress q is ~6 kPa lower (also, the radial and circumferential stresses are not quite equal). These variations are equivalent to those reported from experiments and analyses with triaxial samples consolidated with radial drainage (Carter, 1982; Atkinson, Evans & Ho, 1985; Woods, 1986).

An additional finite element analysis was carried out to investigate the effect of a subsequent load increment, with a vertical stress increment ratio of 0·1, on the non-uniform sample left at the end of the first consolidation step. The results show that at the end of this second consolidation step total variations in specific volume of 0·007, in p' of 8 kPa, and in q of 11 kPa were observed between the middle and the drainage boundaries of the sample. The variations in void ratio, p' and q are to a first approximation cumulative.

The results of an analysis carried out using a vertical stress increment ratio of 0·5 appear to indicate that the rise in excess pore water pressure relative to the applied stress increment (Fig. 3(b)) is independent of the increment ratio. The variations across the sample at the end of consolidation were 0·1 in specfic volume, 70 kPa in p' and 100 kPa in q: the application of large vertical stress increment ratios resulted in considerable non-uniformities at the end of consolidation. Small vertical stress increment ratios should be used if uniformity of samples is required. These finite element analyses are described in detail in Al-Tabbaa (1987).

PRACTICAL IMPLICATIONS

Differential lateral displacements resulting from radial drainage

Consider a hypothetical structure which is circular in plan, with an overall radius of 15 m and some subterranean elements at its centre (such as a service core) which are externally drained, and hence to which water may flow. If the structure is supported on a raft with settlement-reducing piles, a considerable pressure due to the weight of

the building will be exerted on the subsoil, causing a consolidation pattern similar to that shown in Fig. 1. Figure 6 shows that, at radii fairly close to the inner drainage boundary, radial movements occur inwards towards the axis of the problem; however, outward radial movements occur at radii approaching the outer drainage boundary. This suggests that piles at these locations will be subjected to lateral pressures which will tend to force them apart, leading to potential large shear stresses in the pile–slab connections.

If in the prototype $r_0 = 3\ m$ and $V_\infty = 0{\cdot}02$, the maximum horizontal displacement between piles located at radii 5 m and 12 m is almost 30 mm according to the results of the elastic analysis shown in Fig. 6(a), for $T = 0{\cdot}12$. This movement will be reduced in practice by the shear stresses between the soil and the raft. The elastic–plastic analysis may be supposed to represent soil behaviour more accurately; with this analysis the horizontal displacements were only $\sim 20\%$ of the elastic values, so the shear forces at the pile–raft connection may not in fact be particularly large. Buried services installed in brittle pipes may also be damaged by the differential ground distortions resulting from radial consolidation.

Differential vertical settlement

In the analyses performed it has been observed that the vertical stresses at the interface between the soil and the rigid platen become non-uniform during consolidation. In the elastic analysis, the stresses reverted to a uniform state (Fig. 7(a) and (b)), but for the elastic–plastic soil a degree of non-uniformity remained (Fig. 7(c) and (d)). Most structures will in reality be flexible to some extent, and the non-uniform distribution of total vertical stresses that has been computed will be translated in practice into differential settlements. The results shown in Fig. 5 suggest that the total vertical stresses will become higher towards the drainage boundaries. This will lead to hogging distortions at early stages of the consolidation process, which will diminish as consolidation proceeds. In the elastic–plastic analysis the non-uniformity of total vertical stress is much greater than in the elastic analysis. The implied distortion will again be greatest at an early stage of consolidation and will fall with time. At very late stages of the consolidation process the pattern of non-uniformity reverses, so that a transition to sagging distortion may occur.

Many designers will perform consolidation analyses merely to estimate the displacements and distortions that will be present at the end of consolidation. However, the analyses in this Paper indicate that the distortions of a structure may in fact be substantially greater during than after consolidation. The degree of distortion required to cause cracking or structural damage is generally fairly small (Burland & Wroth, 1975). These analytical results suggest that when designing buildings on compressible soil, or when dealing with buildings that are highly susceptible to differential settlement, it may be advisable to analyse the entire consolidation process, with realistic modelling of the actual drainage conditions, in order to discover whether or not any of the distortions caused by radial consolidation are likely to be excessive.

Horizontal drainage may in some situations produce unwelcome ground movements or building distortions. It may be desirable to limit these problems by promoting a predominantly vertical mode of drainage—for example by using a drainage layer, or by attracting water radially over small distances using sand wick drains. Many of the problems mentioned above will thus be minimized.

CONCLUSIONS

Closed-form solutions for the consolidation of an annulus of elastic soil draining radially to concentric inner and outer fixed boundaries can be generated using either an uncoupled analysis, in which all soil elements are assumed to follow the pattern of displacements imposed at the boundary of the sample, or a fully coupled analysis in which the flow of pore water and the changes in effective stress within the soil are linked intimately. The solutions obtained from these two analyses are completely different primarily because the assumptions made in the uncoupled analysis are so far from the actual conditions of the problem that the mathematical result obtained is an incorrect physical result. A first general 'moral' to emerge, therefore, is that even in a problem such as this, where the boundary conditions are apparently simple, the soil deforms inhomogeneously during the consolidation process and analyses which attempt to ignore this inhomogeneity will seriously misrepresent the actual response of the soil. The inhomogeneity is caused by the fact that the direction of pore water flow within the sample is not the same as the direction of imposed overall deformation.

The elastic–plastic finite element analysis using the modified Cam clay model shows effects during the consolidation process that are not exhibited in the elastic analysis, such as initial increase in excess pore water pressure and non-uniformities in stresses and strains across the sample at the end of consolidation. The finite element elastic–plastic analyses suggest that all soil elements across the sample were yielding and following different stress paths during consoli-

dation, and that the strain paths that were followed resulted from the description of soil plasticity that is built into the Cam clay model. The pattern of deformation that occurs within the elastic–plastic soil sample is thus completely different from that observed within the elastic sample. Thus, the second 'moral' to emerge is that non-linearity in soils, which can best be described by plasticity, cannot be ignored. Further, because the equations governing the plastic component of the stress–strain response are quite different from those governing the elastic response, it would not be appropriate to try to describe the soil as an elastic material with a varying stiffness. Similarly, it might appear attractive to deduce an equivalent stiffness from the end of consolidation settlement of the top platen of the oedometer, and then to use this value in a constant stiffness elastic analysis of the settlements that will occur around a geotechnical structure. Such an analysis would give a false indication of the *pattern* of deformations that will occur, even if the stiffness could coincidentally be chosen to match the consolidation settlement at one particular point around the structure.

A more general 'moral' can be drawn from these analyses. It is convenient to think of a conventional vertical-flow oedometer test as a single-element test which produces information on the one-dimensional deformation of a soil. The effective stress state in the sample is not in fact uniform except at the beginning and end of each stage of the consolidation process, but, because of the particular conditions under which the test is run with regard to vertical deformation and drainage, all soil elements within the oedometer sample are forced to follow the same stress–strain relationship, but at different rates depending on their distance from the drainage boundaries. Hence the overall single element interpretation can be justified.

In any three-dimensional problem involving transient pore pressures (the situation studied here is merely a rather simple example of such a problem), the finite length of drainage paths implies that soil elements at different distances from drainage boundaries will follow very different stress and strain paths during the consolidation process. In general, in real soils, as in the elastic–plastic analysis described here, the final condition of the soil mass when consolidation is complete will be inhomogeneous, and a treatment that neglects this inhomogeneity may be seriously in error.

The Cam clay model may or may not be considered to provide an adequate description of the behaviour of any particular real soil. It is certain, however, that a proper analysis of a three-dimensional consolidation problem can only be achieved using a fully coupled effective stress–flow procedure in which the stiffness of the soil is described in a completely general way using an appropriate constitutive model, and in which the flow of pore water is governed by coefficients of permeability which may well be anisotropic and vary with changing specific volume of the soil.

ACKNOWLEDGEMENTS

The work described in this Paper was performed while both Authors were members of the Soil Mechanics Group of Cambridge University Engineering Department. Assistance from other members of the Group and the Department is gratefully acknowledged. The Authors are also grateful to Professor R. E. Gibson and Professor R. L. Schiffman for their comments and advice at various stages of the work.

NOTATION

A, A_n	integration constants
c	coefficient of radial consolidation
C_0, C_1	cylinder functions
D_1, D_2	constants
E	Young's modulus
G	shear modulus
J_0, J_1	Bessel functions of first kind of zeroth and first order
k_h	horizontal permeability
K_{0nc}	coefficient of earth pressure at rest for normally consolidated clay
m_v	coefficient of volume compressibility
M	slope of critical state line in $p' : q$ plane
n	index
p'	mean effective stress $(\sigma_r' + \sigma_\theta' + \sigma_z')/3$
P	total applied load
q	generalized deviator stress $\{[(\sigma_\theta' - \sigma_z')^2 + (\sigma_z' - \sigma_r')^2 + (\sigma_r' - \sigma_\theta')^2]/2\}^{1/2}$
r	radial co-ordinate
r_0	inner radius of sample
R	outer radius of sample
t	time
T	time factor $4ct/[(R - r_0)^2]$
u	pore pressure
U	pore pressure ratio $u/\Delta\bar{\sigma}_z$
v	specific volume
V	volumetric strain
V_∞	volumetric strain at $t = \infty$
x	$\sigma_r' - \sigma_\theta'$
Y_0, Y_1	Bessel functions of second kind of zeroth and first order
z	vertical co-ordinate
γ_w	unit weight of water
Γ	intercept on critical state line in $v : \ln p'$ plane at $p' = 1$ kPa
$\varepsilon_r, \varepsilon_\theta, \varepsilon_z$	radial, circumferential and vertical strains
ε_∞	vertical strain at $t = \infty$
$\dot{\varepsilon}$	vertical strain rate $d\varepsilon_z/dt$
ζ	degree of vertical settlement $\varepsilon_z/\varepsilon_\infty$
θ	circumferential co-ordinate
κ	slope of swelling line in $v : \ln p'$ plane

λ slope of normal compression line in v: ln p' plane
λ_n, μ_n roots of equation (30)
ν Poisson's ratio
ξ radial movement
ρ r/R
$\sigma_r', \sigma_\theta', \sigma_z'$ radial, circumferential and vertical effective stress
$\sigma_r, \sigma_\theta, \sigma_z$ radial, circumferential and vertical total stress
$\bar{\sigma}_z$ average vertical total stress
χ r_0/R

APPENDIX 1. ANALYSES

The boundary conditions which govern the analyses can be described theoretically as follows.

(*a*) The soil is laterally confined so that no radial movement can occur at either the inner or outer boundary

$$\xi(r_0, t) = \xi(R, t) = 0 \tag{1}$$

(*b*) Drainage occurs at the inner and outer boundaries so that the excess pore water pressure at these radii is always zero

$$u(r_0, t) = u(R, t) = 0 \tag{2}$$

(*c*) The soil is contained vertically between rigid platens so that the vertical strain is a function only of time and not of radius

$$\partial\varepsilon_z/\partial r = 0 \tag{3}$$

The vertical strain ε_z is zero at $t = 0$ and tends towards its final value ε_∞ as time increases towards infinity

$$\varepsilon_z(r, 0) = 0, \quad \varepsilon_z(r, \infty) = \varepsilon_\infty$$

(*d*) For all radii, the radial movement, excess pore pressure and vertical strain are initially zero

$$\xi(r, 0-) = u(r, 0-) = \varepsilon_z(r, 0-) = 0$$

(*e*) The consolidation of the sample is driven by an increment of total vertical load ΔP which remains constant with time and whose non-uniform distribution with radius is such that the condition of uniform vertical strain is maintained across the sample. It is convenient to build up the solution in terms of non-dimensional quantities $\rho = r/R$ and $\chi = r_0/R$. This boundary condition can then be written as

$$\int_\chi^1 \rho\Delta\sigma_z \, d\rho = \int_\chi^1 \rho\Delta\sigma_z' \, d\rho + \int_\chi^1 \rho u \, d\rho$$
$$= \Delta P/(2\pi R^2) = (1 - \chi^2)\Delta\bar{\sigma}_z/2 \tag{4}$$

where $\Delta\bar{\sigma}_z$ is the average vertical total stress increment.

Uncoupled analysis. In this analysis the additional assumption is made that movement of soil particles occurs only vertically, governed by a coefficient of volume compressibility m_v

$$\varepsilon_z/\Delta\sigma_z' = m_v \tag{5}$$

$$m_v = (1 + \nu)(1 - 2\nu)/[E(1 - \nu)(1 + \nu)] \tag{6}$$

where ν and E are Poisson's ratio and Young's modulus for the soil skeleton.

The solution is derived in terms of a dimensionless time factor T

$$T = 4ct/[R - r_0)^2] \tag{7}$$

where

$$c = k_h/(m_v\gamma_w) \tag{8}$$

and a dimensionless pore pressure ratio U

$$U = u/\Delta\bar{\sigma}_z \tag{9}$$

and degree of vertical settlement $\zeta = \varepsilon_z/\varepsilon_\infty$.

Combination of the equation of continuity with Darcy's law produces a differential equation linking excess pore pressure u and vertical strain rate $\dot{\varepsilon}$

$$\frac{\partial^2 u}{\partial\rho^2} + \frac{1}{\rho}\frac{\partial u}{\partial\rho} = -(\gamma_w R^2/k_h)\dot{\varepsilon} \tag{10}$$

The vertical strain rate $\dot{\varepsilon} = d\varepsilon_z/dt$ is a function only of time, and hence a soluton of equation (10) satisfying condition (b) above can be found

$$u = (\gamma_w/k_h)(R^2/4)$$
$$\times [(1 - \rho^2) - (1 - \chi^2)(\ln\rho/\ln\chi)]\dot{\varepsilon} \tag{11}$$

From equation (5), as the vertical strain is uniform with radius, the vertical effective stress must also be uniform with radius; combining equations (5) and (11) with condition (*d*) above, a differential equation for $\dot{\varepsilon}$ can be obtained

$$A\dot{\varepsilon} + d\dot{\varepsilon}/dT = 0 \tag{12}$$

where

$$A = \frac{2(1 - \chi)^2 \ln\chi}{[(\chi^2 + 1)\ln\chi + (1 - \chi^2)]} \tag{13}$$

Equation (12) can be solved and combined with condition (*c*) above to give the expression for the average degree of vertical settlement ζ

$$\zeta = \varepsilon_z/\varepsilon_\infty = 1 - e^{-AT} \tag{14}$$

At infinite time the excess pore pressure becomes zero, the total stress is transferred to the effective stress, and, from equation (5), $\varepsilon_\infty = m_v\Delta\bar{\sigma}_z$. Then, integrating equation (14), the strain rate is

$$\dot{\varepsilon} = \frac{cm_v\bar{\sigma}_z}{A} e^{-AT} \tag{15}$$

Finally, combining equations (11) and (15), the variation of pore pressure ratio $U = u/\Delta\bar{\sigma}_z$ with radius and time is

$$U = 2\frac{[(1 - \rho^2)\ln\chi - (1 - \chi^2)\ln\rho]}{[(\chi^2 + 1)\ln\chi + (1 - \chi^2)]} e^{-AT} \tag{16}$$

Note that equation (15) implies that the strain rate is finite and non-zero at time $T = 0$. The response calculated, though mathematically correct given the assumptions that have been made, is not reasonable from an intuitive point of view.

Fully coupled analysis: elastic soil. In this Biot analysis, Hooke's law is used to relate the increments in effective radial, circumferential, and vertical stresses $\Delta\sigma_r'$, $\Delta\sigma_\theta'$, $\Delta\sigma_z'$ and the corresponding strains ε_r, ε_θ, ε_z

$$\begin{bmatrix}\Delta\sigma_r'\\ \Delta\sigma_\theta'\\ \Delta\sigma_z'\end{bmatrix} = E/[(1+\nu)(1-2\nu)] \begin{bmatrix}1-\nu & \nu & \nu\\ \nu & 1-\nu & \nu\\ \nu & \nu & 1-\nu\end{bmatrix}\begin{bmatrix}\varepsilon_r\\ \varepsilon_\theta\\ \varepsilon_z\end{bmatrix} \quad (17)$$

All stresses and strains are assumed to be positive in compression.

The equations of compatibility link radial and circumferential strains ε_r and ε_θ with radial movement ξ

$$\varepsilon_r = -\partial\xi/\partial r \quad (18)$$

$$\varepsilon_\theta = -\xi/r \quad (19)$$

The only non-trivial equation of equilibrium is that describing radial equilibrium, neglecting body forces

$$\frac{\partial\Delta\sigma_r}{\partial r} + (\Delta\sigma_r - \Delta\sigma_\theta)/r = 0 \quad (20)$$

which is written in terms of total radial and circumferential stress increments

$$\Delta\sigma_r = \Delta\sigma_r' + u \quad (21)$$

$$\Delta\sigma_\theta = \Delta\sigma_\theta' + u \quad (22)$$

A flow equation can be written linking radial gradients or pore pressure with time gradients of volumetric strain V in the soil

$$\frac{\partial V}{\partial t} = -\frac{k_h}{\gamma_w}\frac{1}{r}\frac{\partial}{\partial r}\left(r\frac{\partial u}{\partial r}\right) \quad (23)$$

where

$$V = \varepsilon_r + \varepsilon_\theta + \varepsilon_z = -\frac{\partial\xi}{\partial r} - \frac{\xi}{r} + \varepsilon_z \quad (24)$$

Combining equations (18)–(24) gives first

$$(1/m_v)\frac{\partial V}{\partial r} + \frac{\partial u}{\partial r} = 0 \quad (25)$$

and then

$$\frac{1}{r}\frac{\partial}{\partial r}\left(r\frac{\partial V}{\partial r}\right) = \frac{1}{c}\frac{\partial V}{\partial t} \quad (26)$$

where

$$c = k_h E(1-\nu)/\gamma_w[(1+\nu)(1-2\nu)] = k_h/m_v\gamma_w \quad (27)$$

which is the appropriate coefficient of consolidation for this problem.

A solution to these equations satisfying the boundary conditions of the problem can be constructed as follows. A solution of equation (26) can be found in the form

$$V = V_\infty + \sum_{n=1}^{\infty} A_n C_0(\lambda_n\rho)\, e^{-[(1-\chi^2)\lambda_n^2 T/4]} \quad (28)$$

where V_∞ is the volumetric strain at time $T = \infty$, and

$$C_0(\lambda_n\rho) = J_0(\lambda_n\rho) + \mu_n Y_0(\lambda_n\rho) \quad (29)$$

$C_0(\lambda_n\rho)$ are cylinder functions (see, for example, McLachlan (1954)); $J_0(\lambda_n\rho)$ and $Y_0(\lambda_n\rho)$ are Bessel functions of zeroth order of the first and second kind respectively. The values of λ_n and μ_n are roots of the equation

$$\mu_n = -\frac{J_0(\lambda_n\chi)}{Y_0(\lambda_n\chi)} = -\frac{J_0(\lambda_n)}{Y_0(\lambda_n)} \quad (30)$$

The coefficients A_n can be found from the assumption that there is no volumetric strain at time $T = 0$

$$V(\rho, 0) = 0 \quad (31)$$

Then, from equation (28)

$$-V_\infty = \sum_{n=1}^{\infty} A_n C_0(\lambda_n\rho) \quad (32)$$

and hence

$$A_n = -2V_\infty/\{\lambda_n[C_1(\lambda_n) + \chi C_1(\lambda_n\chi)]\} \quad (33)$$

where

$$C_1(\lambda_n\rho) = J_1(\lambda_n\rho) + \mu_n Y_1(\lambda_n\rho) \quad (34)$$

$C_1(\lambda_n\rho)$ are cylinder functions with $J_1(\lambda_n\rho)$ and $Y_1(\lambda_n\rho)$ being Bessel functions of first order of the first and second kind respectively. Equation (28) for the volumetric strain then becomes

$$V/V_\infty = 1 - 2\sum_{n=1}^{\infty}\frac{C_0(\lambda_n\rho)\, e^{-[(1-\chi^2)\lambda_n^2 T/4]}}{\lambda_n[C_1(\lambda_n) + \chi C_1(\lambda_n\chi)]} \quad (35)$$

Now, as the clay is completely confined radially between rigid boundaries at $\rho = \chi$, 1, as the top and bottom boundaries are rigid, and as the pore fluid and the soil particles have been assumed to be incompressible, the uniform vertical strain ε_z at any time is equal to the radial average of the volumetric strain

$$\varepsilon_z = \frac{1}{(1-\chi^2)}\int_\chi^1 2\rho V\, d\rho \quad (36)$$

Substituting from equation (35)

$$\varepsilon_z/V_\infty = 1 - \frac{4}{(1-\chi^2)}\sum_{n=1}^{\infty}\frac{D_1\, e^{-[(1-\chi^2)\lambda_n^2 T/4]}}{\lambda_n^2 D_2} \quad (37)$$

where

$$D_1 = C_1(\lambda_n) - \chi C_1(\lambda_n\chi) \quad (38)$$

$$D_2 = C_1(\lambda_n) + \chi C_1(\lambda_n\chi) \quad (39)$$

From equations (18), (19) and (24)

$$V - \varepsilon_z = \varepsilon_r + \varepsilon_\theta = -\frac{1}{r}\frac{\partial}{\partial r}(r\xi) \quad (40)$$

Substituting for V and ε_z from equations (35) and (37) and integrating gives the outward radial movement ξ

$$\xi/(RV_\infty) = 2\sum_{n=1}^{\infty}[C_1(\lambda_n\rho) - \rho D_1/(1-\chi^2)] \times e^{-[(1-\chi^2)\lambda_n^2 T/4]}/(\lambda_n^2 D_2) + f(t)/\rho \quad (41)$$

The function f(t) can be deduced from equation (1)

$$f(t) = \frac{2\chi}{(1-\chi^2)} \sum_{n=1}^{\infty} [\chi C_1(\lambda_n) - C_1(\lambda_n \chi)] \times e^{-[(1-\chi^2)\lambda_n^2 T/4]/(\lambda_n^2 D_2)} \quad (42)$$

It remains to find the pore pressure u from equation (21)

$$u = -V/m_v + g(t) \quad (43)$$

and the functon g(t) can be deduced from equations (2) and (30)

$$g(t) = V_\infty/m_v \quad (44)$$

Hence

$$u = (2V_\infty/m_v) \sum_{n=1}^{\infty} C_0(\lambda_n \rho)\, e^{-[(1-\chi^2)\lambda_n^2 T/4]/(\lambda_n D_2)} \quad (45)$$

The final unknown quantity is V_∞, the ultimate value of the volumetric strain. This can be determined from equation (4). From equations (17) and (40)

$$\Delta\sigma_z' = [E/(1+\nu)]\{[\nu/(1-2\nu)]V + \varepsilon_z\} \quad (46)$$

and equation (4) becomes

$$\Delta P/(2\pi R^2) = [E/(1+\nu)]\left\{[\nu/(1-2\nu)] \times \int_\chi^1 \rho V \, d\rho + \int_\chi^1 \rho\varepsilon_z \, d\rho\right\} + \int_\chi^1 \rho u \, d\rho \quad (47)$$

Hence, from equation (36)

$$\Delta P/(2\pi R^2) = (1/m_v)(1-\chi^2)\varepsilon_z/2 + \int_\chi^1 \rho u \, d\rho \quad (48)$$

and substituting from equations (38), (46) and (4) it finally emerges that

$$V_\infty = \Delta\bar{\sigma}_z m_v \quad (49)$$

indicating that the final volumetric compressive strain is the same as that caused by the average total vertical stress increment $\Delta\bar{\sigma}_z$, using the appropriate compliance $m_v = (1+\nu)(1-2\nu)/[E(1-\nu)]$.

APPENDIX 2. DETAILS OF THE FINITE ELEMENT ANALYSES

The initial vertical effective stress was chosen to be $\sigma_z' = 300$ kPa. To impose conditions of one-dimensional vertical consolidation, a value for the coefficient of lateral earth pressure K_{0nc} of 0·78 computed from the modified Cam clay model was used, giving a value of 231 kPa for the initial horizontal effective stress and a value of 254 kPa for the mean effective stress p'.

The properties assigned to the soil in the two types of analyses performed are given below. In the elastic analysis Young's modulus $E = 1070$ kPa was chosen. This value was obtained by combining the value of the bulk modulus on the one-dimensional normal compression line, calculated experimentally at the stress state considered here, with a Poisson's ratio of $\nu = 0{\cdot}435$, which corresponds to $K_{0nc} = 0{\cdot}78$. The corresponding value of the shear modulus is $G = 372$ kPa. Values of the vertical and horizontal permeabilities of $0{\cdot}7 \times 10^{-6}$ mm/s and $1{\cdot}86 \times 10^{-6}$ mm/s respectively were chosen from experimental results. These permeability values are obtained experimentally for $p' = 254$ kPa, which corresponds to a specific volume $v = 2{\cdot}15$.

In the elastic–plastic analysis the following properties were chosen for the soil based on experimental work (see Al-Tabbaa (1987)): the slope of the normal compression line in the $v : \ln p'$ plane $\lambda = 0{\cdot}18$; the initial slope of the swelling line in the same plane $\kappa = 0{\cdot}015$; the specific volume on the critical state line at $p' = 1$ kPa $\Gamma = 3{\cdot}0$; the slope of the critical state line in the $p' : q$ plane $M = 0{\cdot}9$; and Poisson's ratio $\nu = 0{\cdot}3$. The same permeability values were used as in the elastic analysis.

REFERENCES

Al-Tabbaa, A. (1987). *Permeability and stress–strain response of speswhite kaolin.* PhD thesis, University of Cambridge.

Al-Tabbaa, A. & Wood, D. M. (1987). Some measurements of the permeability of kaolin. *Géotechnique* **37**, No. 4, 499–503.

Atkinson, J. H., Evans, J. S. & Ho, E. W. L. (1985). Non-uniformity of triaxial samples due to consolidation with radial drainage. *Géotechnique* **35**, No. 3, 353–356.

Barron, R. A. (1948). Consolidation of fine-grained soils by drain wells. *Trans. Am. Soc. Civ. Engrs* **113**, 718–742.

Britto, A. M. & Gunn, M. J. (1987). *Critical state soil mechanics via finite elements.* Chichester: Ellis Horwood.

Burland, J. B. & Wroth, C. P. (1975). Settlement of buildings and associated structures. *Proc. Conf. on Settlement of Structures, Cambridge*, pp. 611–654. London: Pentech Press.

Carslaw, H. S. & Jaeger, J. C. (1959). *Conduction of heat in solids*, 2nd edn. Oxford: Clarendon Press.

Carter, J. P. (1982). Predictions of the non-homogeneous behaviour of clay in the triaxial text. *Géotechnique* **32**, No. 1, 55–58.

McKinlay, D. G. (1961). A laboratory study of rates of consolidation in clays with particular reference to conditions of radial porewater drainage. *Proc. 5th Int. Conf. Soil Mech. Fdn Engng, Paris*, Vol. 1, pp. 225–228.

McLachlan, N. W. (1954). *Bessel functions for engineers*, 2nd edn. Oxford: Clarendon Press.

Randolph, M. F. & Carter, J. P. (1979). The effect of pile permeability on the stress changes around a pile driven into clay. *Proc. 3rd Int. Conf. Numer. Meth. Geomech., Aachen*, pp. 1097–1105.

Randolph, M. F. & Wroth, C. P. (1979). An analytical solution for the consolidation around a driven pile. *Int. J. Numer. Analyt. Meth. Geomech.* **3**, 217–229.

Roscoe, K. H. & Burland, J. B. (1968). On the generalised stress–strain behaviour of 'wet' clay. *Engineering plasticity* (edited by J. Heyman & F. A. Leckie), pp. 535–609. Cambridge University Press.

Wood, D. M. (1984). On stress parameters. *Géotechnique* **34**, No. 2, 282–287.

Wood, D. M. (1991). *Soil behaviour and critical state soil mechanics.* Cambridge University Press.

Woods, R. I. (1986). Finite element analysis of coupled loading and consolidation. *Proc. 2nd Int. Symp. Numer. Models Geomech., Ghent*, pp. 709–718.